Distributed Controllers for Human-Robot Locomotion: A Scalable Approach Based on Decomposition and Hybrid Zero Dynamics

Vinay R. Kamidi, Jonathan C. Horn, Robert D. Gregg, and Kaveh Akbari Hamed

***Abstract*— This paper presents a formal foundation, based on decomposition, hybrid zero dynamics (HZD), and a scalable optimization, to develop distributed control algorithms for hybrid models of collaborative human-robot locomotion. The proposed approach considers a centralized controller and then decomposes the dynamics and feedback laws with a parameterization to synthesize local controllers. The Jacobian matrix of the Poincaré map with local controllers is studied and compared to that with centralized ones. An optimization problem is then set up to tune the parameters of the local controllers for asymptotic stability. The proposed approach can significantly reduce the number of controller parameters to be optimized for the synthesis of distributed controllers. The analytical results are numerically evaluated with simulations of a multi-domain hybrid model with 19 degrees of freedom for stable amputee locomotion with a powered knee-ankle prosthetic leg.**

***Index Terms*— Distributed Control, Stability of Hybrid Systems, Robotics.**

I. Introduction

COOPERATIVE human-robot locomotion is a complex problem as by nature, the human and prosthesis act as individual subsystems— this motivates the development of decentralized/distributed controllers to effectively coordinate the action of subsystems. State-of-the-art feedback controllers for autonomous legged locomotion are mainly tailored to centralized techniques that have *no* provision to consider decentralized walking models. Although decentralized controllers have recently been developed for powered prostheses, existing techniques mainly focus on the development of linear and time-varying local controllers, see e.g., [1], [2]. These techniques require different parameters at different time periods to be tuned to account for the nonlinear dynamics in locomotion. This results in clinicians spending significant time in tuning control parameters [3] for each individual. These roadblocks *motivate* the development of a class of nonlinear distributed controllers that consider the independent nature of the human and prosthesis systems and thus facilitate a reduction in the number of parameters.

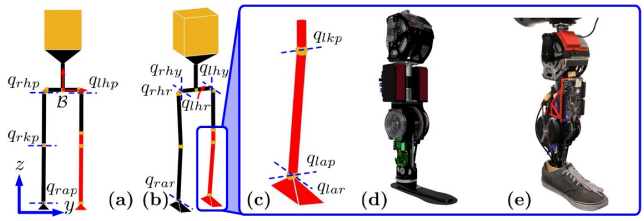

Fig. 1. (a) Front and (b) isometric views illustrating all joints in the human subsystem. (c) Isometric view showing joints in the robotic subsystem. (d) CAD illustration of the robot. (e) Assembled powered prosthesis.

Hybrid systems theory has become a powerful approach for modeling legged locomotion [4]–[10]. Existing nonlinear control approaches that address the hybrid nature of locomotion are tailored to centralized techniques, such as hybrid reduction [11], [12], controlled symmetries [6], transverse linearization [7], [13], and Hybrid Zero Dynamics (HZD) [14]. The use of distributed/decentralized control is extensively observed in large-scale systems, e.g., power systems [15] and network systems [16]. Moreover, the wealth of research on decentralization is tailored to the stabilization of equilibrium points in ordinary differential equations (ODEs) but *not* periodic orbits (i.e., gaits) of hybrid models of locomotion [17].

Recently, in [18], distributed controllers were extended to exoskeletons but does not consider the interaction forces. References [19]–[21] presented nonlinear local controllers for powered prostheses based on the availability of force measurements to capture the strong interaction between the subsystems. In [22], [23], we introduced nonlinear decentralized control schemes that do not require any force measurements but still consider the interaction amongst the subsystems. Here, the decentralized controllers are synthesized by setting up a large-scale optimization problem based on an iterative sequence of bilinear matrix inequalities (BMIs) for a bipedal model with point feet. The BMI algorithm develops local controllers from scratch by optimizing for a significant amount of controller parameters. This may result in a computational bottleneck for multi-domain locomotion models with nontrivial feet and high degrees of freedom (DOFs). In our most recent work [24], we explored an alternative approach, based on decomposition, towards decentralization for quadrupedal locomotion.

The work of V. Kamidi and J. Horn is supported by the National Science Foundation (NSF) under the Grant 1854898. The work of K. Akbari Hamed is supported by the NSF under Grant 1923216. R. Gregg holds a Career Award at the Scientific Interface from the Burroughs Wellcome Fund.

V. R. Kamidi and K. Akbari Hamed are with the Department of Mechanical Engineering, Virgina Tech, Blacksburg, VA, 24061, USA, {vinay28, kavehakbarihamed}@vt.edu

J. C. Horn is with the Department of Mechanical Engineering and Department of Bioengineering, University of Texas at Dallas, Richardson, TX 75080, USA, jch160630@utdallas.edu

R. D. Gregg is with the Department of Electrical Engineering and Computer Science and the Robotics Institute, University of Michigan, Ann Arbor, MI 48109, USA, rdgregg@umich.edu

This approach presumes the existence of an orbit stabilized by centralized controllers from which local controllers are synthesized with fewer design parameters. In particular, we showed through numerical simulations that decomposition is a feasible approach but did *not* provide any formal foundations and considered the problem *only* for symmetric quadrupedal systems.

The *overarching goal* of this paper is to present a systematic and scalable approach, based on decomposition, HZD, and optimization, to develop nonlinear distributed controllers that exponentially stabilize collaborative human-robot locomotion with asymmetric models. The *contributions* and *key objectives* of this paper are as follows: (1) We propose a decomposition approach for the synthesis of distributed controllers. The integration of decomposition and optimization allows for a significant reduction of the parametric space as we only need to modify and optimize the already-existing centralized HZD controller rather than searching for local controllers from scratch. This leads to a small-scale optimization problem. (2) We study the properties of the Jacobian of the Poincaré map of the centralized and distributed controllers and show that there exists an upper bound on the norm of the difference of Jacobian matrices that significantly simplifies the search for optimal local control parameters. (3) We numerically validate the analytical foundation by designing distributed controllers for multi-domain and collaborative human-robot locomotion with a powered knee-ankle prosthetic leg and nontrivial feet, having a total of 19 DOFs (see Fig. 1). We show that the proposed approach can effectively synthesize local controllers for this comprehensive model of locomotion. In particular, we reduce the number of local controller parameters to be tuned and optimized to almost 5.2% of that in [22].

II. Hybrid Model of Locomotion

In this section, we consider single-domain hybrid models of locomotion to simplify the development of distributed control algorithms. The result can, however, be extended to multi-domain hybrid models of locomotion. We assume that the generalized coordinates of the mechanical system can be given by $q \in \mathcal{Q} \subset \mathbb{R}^{n_q}$. The state vector is also chosen as $x := \text{col}(q, \dot{q}) \in \mathcal{X} \subset \mathbb{R}^n$, in which "col" denotes the column operator, $n = 2\,n_q$, and $\mathcal{X} := \text{T}\mathcal{Q} := \mathcal{Q} \times \mathbb{R}^{n_q}$ represents the state manifold. The control inputs (i.e., torques) to the system are represented by $u \in \mathcal{U} \subset \mathbb{R}^m$. The guard of the hybrid system is represented by the $(n-1)$-dimensional manifold $\mathcal{S}$ on which the state trajectory undergoes an abrupt change according to impact dynamics [25]. The open-loop hybrid model of locomotion can be then expressed as follows:

$$\Sigma^{\text{ol}} : \begin{cases} \dot{x} = f(x) + g(x)\,u, & x \in \mathcal{X} \\ x^+ = \Delta(x^-), & x^- \in \mathcal{X} \cap \mathcal{S}, \end{cases} \tag{1}$$

where x^- and x^+ denote the state of the system right before and right after the discrete-time transition, respectively, $\Delta : \mathcal{X} \to \mathcal{X}$ is a smooth (i.e., $\mathcal{C}^\infty$) reset map, and f and g are smooth functions. The equations of motion can be described by

$$D(q)\,\ddot{q} + H\,(q, \dot{q}) = B(q)\,u, \tag{2}$$

in which $D(q) \in \mathbb{R}^{n_q \times n_q}$ is the mass-inertia matrix, $H(q, \dot{q}) \in \mathbb{R}^{n_q}$ represents the Coriolis, centrifugal, and gravitational terms, and $B(q) \in \mathbb{R}^{n_q \times m}$ is the input matrix.

Assumption 1: (Periodic Orbit and Phasing Variable): There exists a *periodic solution* (i.e., gait) to the hybrid model (1) for some nominal control inputs and some fundamental period $T^\star > 0$. The corresponding *periodic orbit* is represented by $\mathcal{O} \subset \mathcal{X}$. To define the desired evolution of the state and control inputs on $\mathcal{O}$, we make use of a time-based *phasing variable* as $\tau := \frac{t - t^+}{T^\star}$, where t^+ represents the time sample right after the discrete-time event. The evolution of the state and control inputs on $\mathcal{O}$ are further denoted by $x^\star(\tau) := \text{col}(q^\star(\tau), \dot{q}^\star(\tau))$ and $u^\star(\tau)$ for $0 \le \tau < 1$.

We next present an HZD-based centralized controller to exponentially stabilize the desired orbit $\mathcal{O}$ for the hybrid model of locomotion. For this purpose, we make use of the following time-varying holonomic outputs (i.e., virtual constraints) to be imposed

$$y(\tau, q) := C\,(q - q^\star(\tau))\,, \tag{3}$$

for some full-rank output matrix C with the property $\dim(y) \le \dim(u)$. We are interested in the desired output dynamics $\ddot{y} + k_d\,\dot{y} + k_p\,y = 0$ for some positive gains k_p and k_d. Employing the standard input-output (I-O) linearization [26] yields the following centralized controller

$$u = \Gamma(\tau, x) := -\,(\text{L}_g\text{L}_f y)^\dagger \left(\text{L}_f^2 y + \frac{\partial^2 y}{\partial \tau^2}(\dot{\tau})^2 + k_d\,\dot{y} + k_p\,y\right), \tag{4}$$

that results in $\lim_{t\to\infty} y(t) = 0$, where $(\text{L}_g\text{L}_f y)^\dagger$ denotes the Moore–Penrose inverse of the decoupling matrix $\text{L}_g\text{L}_f y$.

III. Distributed Feedback Controllers

This section develops distributed feedback controllers, based on the decomposition approach, to exponentially stabilize the periodic orbit $\mathcal{O}$ (see Fig. 2(c)). We consider the synthesis problem of local controllers for two subsystems of the hybrid model of locomotion (1). Without loss of generality, we assume that the generalized coordinate vector and control inputs can be decomposed as $q = \text{col}(q_1, q_2)$ and $u = \text{col}(u_1, u_2)$, where $q_i \in \mathcal{Q}_i$ and $u_i \in \mathcal{U}_i$ denote the local configuration variables and local control inputs for the subsystem Σ_i for $i \in \{1, 2\}$. The local state variables are further denoted by $x_i := \text{col}(q_i, \dot{q}_i) \in \mathcal{X}_i$.

1) Decomposition Approach: To develop local controllers, we make the following assumption.

Assumption 2: (State Approximation for Subsystems): We suppose that the subsystem Σ_i for every $i \in \{1, 2\}$ can approximate the state variables for the other subsystem, i.e. Σ_j, $j \neq i \in \{1, 2\}$, by their desired values on the periodic orbit $\mathcal{O}$, that is, $x_j \approx x_j^\star(\tau)$.

We then decompose the equations of motion in (2) as

$$D_{ii}\,\ddot{q}_i + D_{ij}\,\ddot{q}_j + H_i = B_{ii}\,u_i + B_{ij}\,u_j \tag{5}$$

for all $i \neq j \in \{1, 2\}$. From (5), one can solve for $\ddot{q}_i$, i.e.,

$$\begin{aligned} &\left(D_{ii} - D_{ij}\,D_{jj}^{-1}\,D_{ji}\right)\ddot{q}_i + H_i - D_{ij}\,D_{jj}^{-1}\,H_j = \\ &\left(B_{ii} - D_{ij}\,D_{jj}^{-1}B_{ji}\right)u_i + \left(B_{ij} - D_{ij}\,D_{jj}^{-1}\,B_{jj}\right)u_j. \end{aligned} \tag{6}$$

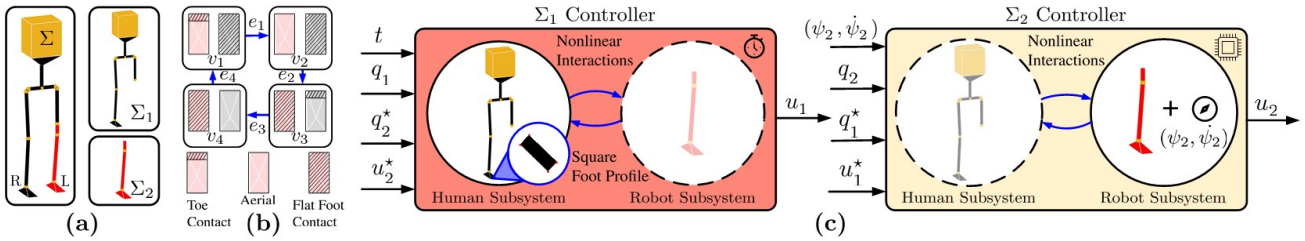

Fig. 2. Illustration depicting (a) the decomposition of the human-robot system ($\boldsymbol{\Sigma}$) into two distinct subsystems: human ($\boldsymbol{\Sigma_1}$), and robot ($\boldsymbol{\Sigma_2}$). (b) Four-domain directed graph representing the gait. (c) Graphical elaboration of the distributed control synthesis based on the decomposition approach.

Using Assumption 2, the nonlinear dynamics for subsystem i can be approximated as follows:

$$\bar{D}_{ii}\left(q_i,t\right)\ddot{q}_i+\bar{H}_i\left(q_i,\dot{q}_i,t\right)=\bar{B}_{ii}\left(q_i,t\right)u_i, \tag{7}$$

in which $\bar{D}_{ii} := D_{ii} - D_{ij}\,D_{jj}^{-1}\,D_{ji}$, $\bar{H}_i := H_i - D_{ij}\,D_{jj}^{-1}\,H_j - (B_{ij} - D_{ij}\,D_{jj}^{-1}\,B_{jj})\,u_j$, and $\bar{B}_{ii} := B_{ii} - D_{ij}\,D_{jj}^{-1}B_{ji}$ that are evaluated at $q_j = q_j^\star(\tau)$, $\dot{q}_j = \frac{\partial q_j^\star}{\partial \tau}(\tau)\,\dot{\tau}$, and $u_j = u_j^\star(\tau)$. Furthermore, the subsystem i can approximate the nonlinear dynamics of the other subsystem, i.e., the subsystem j, as

$$\bar{D}_{jj}\left(q_i,t\right)\ddot{q}_j+\bar{H}_j\left(q_i,\dot{q}_i,t\right)=\bar{B}_{ji}\left(q_i,t\right)u_i, \tag{8}$$

where $\bar{D}_{jj} := D_{jj} - D_{ji}\,D_{ii}^{-1}\,D_{ij}$, $\bar{H}_j = H_j - D_{ji}\,D_{ii}^{-1}\,H_i - (B_{jj} - D_{ji}\,D_{ii}^{-1}\,B_{ij})\,u_j$, and $\bar{B}_{ji} := B_{ji} - D_{ji}\,D_{ii}^{-1}\,B_{ii}$ evaluated at $q_j = q_j^\star(\tau)$, $\dot{q}_j = \frac{\partial q_j^\star}{\partial \tau}(\tau)\,\dot{\tau}$, and $u_j = u_j^\star(\tau)$.

2) Output Modification and Local Controllers: The virtual constraints (3) can be decomposed as $y = \mathrm{col}(y_1, y_2)$ for some local outputs y_1 and y_2 with the property $\dim(y_i) \leq \dim(u_i)$, $i \in \{1,2\}$. In particular, we assume that

$$y_i = C_{ii}\left(q_i - q_i^\star(\tau)\right) + C_{ij}\left(q_j - q_j^\star(\tau)\right) \tag{9}$$

for all $i \neq j \in \{1,2\}$. Using Assumption 2, the local output y_i can be reduced to $y_i = C_{ii}\left(q_i - q_i^\star(\tau)\right)$. Our previous work [22] showed that such local virtual constraints may *not* stabilize the orbit $\mathcal{O}$ for the hybrid model of locomotion. To tackle this challenge, we make the following assumption.

Assumption 3: (Measurable Global Variables): We suppose that there are some smooth functions $\psi_i(x) = \psi_i(x_1, x_2)$, referred to as *measurable global variables*, that 1) depend on the global states x_1 and x_2, and 2) are measurable for the subsystem Σ_i along the trajectories of the hybrid model via some sensors.

We next consider some measurable holonomic global variables for the subsystem i represented by $\psi_i(q)$. We further suppose that both ψ_i and $\dot{\psi}_i$ are measurable for the subsystem Σ_i. Our motivation for this assumption comes from the fact that robotic prosthetic legs can be equipped with some inertial measurements units (IMUs) attached to the human thigh to measure the absolute position and velocity variables that depend on the global states $(q, \dot{q})$. We then modify the local output for the subsystem Σ_i as follows:

$$y_i = C_{ii}\left(q_i - q_i^\star(\tau)\right) + E_i\left(\psi_i(q) - \psi_i^\star(\tau)\right), \tag{10}$$

where $\psi_i^\star(\tau)$ denotes the desired evolution of the measurable global variables ψ_i on $\mathcal{O}$ in terms of the phasing variable τ. The local output (10) is further parameterized by an output matrix E_i to be determined in Section IV. Differentiating the output (10) results in

$$\begin{aligned}\ddot{y}_i = C_{ii}&\left(\ddot{q}_i - \frac{\partial^2 q_i^\star}{\partial \tau^2}\left(\dot{\tau}\right)^2\right)\\ &+ E_i\left(\frac{\partial \psi_i}{\partial q}\ddot{q} + \frac{\partial}{\partial q}\left(\frac{\partial \psi_i}{\partial q}\dot{q}\right)\dot{q} - \frac{\partial^2 \psi_i^\star}{\partial \tau^2}(\dot{\tau})^2\right),\end{aligned} \tag{11}$$

in which the acceleration terms, i.e., $\ddot{q}_i$ and $\ddot{q} = \mathrm{col}(\ddot{q}_1, \ddot{q}_2)$, can be approximated using the nonlinear dynamics (7) and (8). Furthermore, the nonlinear terms $\frac{\partial \psi_i}{\partial q}$ and $\frac{\partial}{\partial q}(\frac{\partial \psi_i}{\partial q}\,\dot{q})\,\dot{q}$ can be computed utilizing Assumption 2. This would result in an input-affine output dynamics as follows:

$$\ddot{y}_i = A_i\left(\tau, x_i\right)u_i + b_i\left(\tau, x_i\right) = -k_d\,\dot{y}_i - k_p\,y_i. \tag{12}$$

From the output dynamics (12), one can solve for the minimum 2-norm local control solution, that is,

$$u_i = \Gamma_i(\tau, x_i, \psi_i, \dot{\psi}_i) := -A_i^\dagger\left(b_i + k_d\,\dot{y}_i + k_p\,y_i\right). \tag{13}$$

IV. Exponential Stability Analysis

This section investigates the exponential stabilization problem of the periodic orbit $\mathcal{O}$ under the proposed HZD-based distributed feedback controllers (13). We study the Jacobian matrix of the Poincaré map with distributed controllers and then set up an optimization-based approach to tune the parameters of the local controllers.

A. Poincaré Sections Analysis for Closed-Loop Systems

The evolution of the closed-loop mechanical system with centralized and distributed feedback controllers can be expressed by the following hybrid models

$$\Sigma^{\mathrm{cl}}: \begin{cases} \begin{bmatrix}\dot{x}\\ \dot{\tau}\end{bmatrix} = \begin{bmatrix} f^{\mathrm{cl}}\left(\tau, x\right)\\ \frac{1}{T^\star}\end{bmatrix}, & x \in \mathcal{X}\\ \begin{bmatrix}x^+\\ \tau^+\end{bmatrix} = \begin{bmatrix}\Delta\left(x^-\right)\\ 0\end{bmatrix}, & x^- \in \mathcal{X} \cap \mathcal{S}\end{cases} \tag{14}$$

and

$$\hat{\Sigma}^{\mathrm{cl}}: \begin{cases} \begin{bmatrix}\dot{x}\\ \dot{\tau}\end{bmatrix} = \begin{bmatrix} \hat{f}^{\mathrm{cl}}\left(\tau, x\right)\\ \frac{1}{T^\star}\end{bmatrix}, & x \in \mathcal{X}\\ \begin{bmatrix}x^+\\ \tau^+\end{bmatrix} = \begin{bmatrix}\Delta\left(x^-\right)\\ 0\end{bmatrix}, & x^- \in \mathcal{X} \cap \mathcal{S},\end{cases} \tag{15}$$

where $\hat{\Gamma}(\tau, x) := \mathrm{col}(\Gamma_1(\tau, x_1, \psi_1, \dot{\psi}_1), \Gamma_2(\tau, x_2, \psi_2, \dot{\psi}_2))$ represents the distributed controllers, and $f^{\mathrm{cl}}(\tau, x) := f(x) + g(x)\,\Gamma(\tau, x)$ and $\hat{f}^{\mathrm{cl}}(\tau, x) := f(x) + g(x)\,\hat{\Gamma}(\tau, x)$ denote the closed-loop vector fields with centralized and distributed feedback laws, respectively. For future purposes, we define

the augmented states as $x_a := \text{col}(x, \tau) \in \mathcal{X}_a := \mathcal{X} \times \mathbb{R}_+$, augmented vector fields as $f_a^{\text{cl}}(x_a) := \text{col}(f^{\text{cl}}(\tau, x), \frac{1}{T^\star})$ and $\hat{f}_a^{\text{cl}}(x_a) := \text{col}(\hat{f}^{\text{cl}}(\tau, x), \frac{1}{T^\star})$, augmented reset law as $\Delta^{\text{cl}}(x_a) := \text{col}(\Delta(x), 0)$, and $\mathcal{S}_a := \mathcal{S} \times \mathbb{R}_+$. We then denote the Poincaré maps for the closed-loop hybrid models (14) and (15) by $P_a : \mathcal{S}_a \to \mathcal{S}_a$ and $\hat{P}_a : \mathcal{S}_a \to \mathcal{S}_a$, respectively.

Lemma 1: (Fixed Points): Under Assumptions 1-3, $x_{af}^\star := \text{col}(x_f^\star, 1)$ is a fixed point for the Poincaré maps, i.e., $P_a(x_{af}^\star) = \hat{P}_a(x_{af}^\star) = x_{af}^\star$, where $x_f^\star := x^\star(1) = \overline{\mathcal{O}} \cap \mathcal{S}$.

The proof is immediate according to the construction procedure. From Lemma 1, $\mathcal{O}_a := \{(x, \tau) \,|\, x = x^\star(\tau),\, 0 \le \tau < 1\}$ is a periodic orbit for the closed-loop hybrid systems (14) and (15). Let us denote the time evolution of the augmented state trajectory along $\overline{\mathcal{O}}_a$ (i.e., the closure of $\mathcal{O}_a$) by $x_a^\star(t)$ for $0 \le t \le T^\star$. We then define the Jacobian matrices of the augmented vector fields along $x_a^\star(t)$ by $A(t)$ and $\hat{A}(t)$, that is, $A(t) := \frac{\partial f_a^{\text{cl}}}{\partial x_a}(x_a^\star(t))$ and $\hat{A}(t) := \frac{\partial \hat{f}_a^{\text{cl}}}{\partial x_a}(x_a^\star(t))$ for $t \in [0, T^\star]$. We now make the following assumption.

Assumption 4: There are $L > 0$ and $\mu > 0$ such that for all $t \in [0, T^\star]$, $\|A(t)\|_2 \le L$ and $\|A(t) - \hat{A}(t)\|_2 \le \mu$.

Lemma 2: (Variational Equations): Under Assumptions 1-4, consider $\dot{\Phi}(t) = A(t)\,\Phi(t)$ and $\dot{\hat{\Phi}}(t) = \hat{A}(t)\,\hat{\Phi}(t)$ for $t \in [0, T^\star]$ with $\Phi(0) = \hat{\Phi}(0) = I$. Let us define $\varphi(t) := \text{vec}(\Phi(t))$ and $\hat{\varphi}(t) := \text{vec}(\hat{\Phi}(t))$, where the "vec" denotes the vectorization operator. Then, there is $\delta > 0$ such that for all $t \in [0, T^\star]$, $\|\varphi(t) - \hat{\varphi}(t)\|_2 \le \frac{\mu\,\delta}{L}\,(\exp(L\,t) - 1)$.

Proof: From properties of the vectorization operator, $\dot{\varphi} = \text{vec}(A(t)\,\Phi) = (I \otimes A(t))\,\text{vec}(\Phi) = (I \otimes A(t))\,\varphi$, and similarly, $\dot{\hat{\varphi}} = (I \otimes \hat{A}(t))\,\hat{\varphi}$, where "$\otimes$" denotes the Kronecker product. Furthermore, we can show that $\|I \otimes A(t)\|_2 = \|A(t)\|_2 \le L$ and $\|I \otimes A(t) - I \otimes \hat{A}(t)\|_2 = \|A(t) - \hat{A}(t)\|_2 \le \mu$ for all $t \in [0, T^\star]$. These properties together with $\varphi(0) = \hat{\varphi}(0) = \text{vec}(I)$, boundedness of the solutions, i.e., $\exists\ \delta > 0$ such that $\|\varphi(t)\|_2 \le \delta$ and $\|\hat{\varphi}(t)\|_2 \le \delta$ for $t \in [0, T^\star]$, and applying [27, Theorem 3.4, pp. 96] to the ODEs complete the proof. ∎

We are now in a position to present the following theorem.

Theorem 1: (Upper Bound on the Norm of the Difference of the Jacobian Matrices): Under Assumptions 1-4, there is a constant $\beta > 0$ such that

$$\left\| \frac{\partial P_a}{\partial x_a}\left(x_{af}^\star\right) - \frac{\partial \hat{P}_a}{\partial x_a}\left(x_{af}^\star\right) \right\|_2 \le \frac{\mu\,\beta}{L}\left(\exp(L\,T^\star) - 1\right).$$

Proof: From [28, Theorem 1] and [29, Appendix D], the Jacobian linearization of the Poincaré return maps can be given by $\frac{\partial P_a}{\partial x_a}(x_{af}^\star) = \Pi\,\Phi(T^\star)\,\frac{\partial \Delta_a}{\partial x_a}(x_{af}^\star)$ and $\frac{\partial \hat{P}_a}{\partial x_a}(x_{af}^\star) = \Pi\,\hat{\Phi}(T^\star)\,\frac{\partial \Delta_a}{\partial x_a}(x_{af}^\star)$, where Π is the saltation matrix, defined by $\Pi := I - 1/(\frac{\partial s_a}{\partial x_a}(x_{af}^\star)\,f_a^{\text{cl}}(x_{af}^\star))\,f_a^{\text{cl}}(x_{af}^\star)\,\frac{\partial s_a}{\partial x_a}(x_{af}^\star)$. Here, we assume that the augmented switching manifold $\mathcal{S}_a$ can be expressed as the zero-level set of the switching function $s_a(x_a)$. From Lemma 1, $f_a^{\text{cl}}(x_{af}^\star) = \hat{f}_a^{\text{cl}}(x_{af}^\star)$, and hence, Π is indeed the saltation matrix for both Jacobian matrices. From the properties of the vectorization operator, there is a scalar $\gamma > 0$ such that $\|\Phi(T^\star) - \hat{\Phi}(T^\star)\| \le \gamma\|\varphi(T^\star) - \hat{\varphi}(T^\star)\|$ which in combination with Lemma 2 and norm properties results in $\|\frac{\partial P_a}{\partial x_a}(x_{af}^\star) - \frac{\partial \hat{P}_a}{\partial x_a}(x_{af}^\star)\| \le \|\Pi\|\|\frac{\partial \Delta_a}{\partial x_a}(x_{af}^\star)\|\frac{\mu\,\delta\,\gamma}{L}(\exp(L\,T^\star) - 1)$. Finally, defining $\beta := \delta\,\gamma\,\|\Pi\|\|\frac{\partial \Delta_a}{\partial x_a}(x_{af}^\star)\|$ completes the proof. ∎

B. Distributed Controller Synthesis

In order to synthesize distributed controllers, we look for some output matrices E_i, $i \in \{1, 2\}$ in (10) to exponentially stabilize $\mathcal{O}$ via proposed local controllers. For this purpose, let us denote the columns of E_i by ξ_i, that is, $\xi_i := \text{vec}(E_i)$. The local controllers Γ_i in (13) can be then represented by *parameterized feedback laws* $\Gamma_i(\tau, x_i, \psi_i, \dot{\psi}_i, \xi_i)$. We further define the control parameters as $\xi := \text{col}(\xi_1, \xi_2)$. This allows us to parameterize the Jacobian matrix of the Poincaré map by ξ which can be denoted by $\frac{\partial \hat{P}_a}{\partial x_a}(x_{af}^\star, \xi)$. The exponential stabilization problem then consists of finding the controller parameters ξ such that the eigenvalues of $\frac{\partial \hat{P}_a}{\partial x_a}(x_{af}^\star, \xi)$ strictly lie inside the unit circle. We then set up a nonlinear program (NLP) to look for stabilizing parameters ξ as follows:

$$\begin{aligned} \min_{\xi} \quad & \frac{1}{2}\|\xi\|_2^2 \\ \text{s.t.} \quad & \left| \text{eig}\left(\frac{\partial \hat{P}_a}{\partial x_a}\left(x_{af}^\star, \xi\right) \right) \right| < 1. \end{aligned} \tag{16}$$

Here, we search for the minimum 2-norm controller parameters to make modified outputs (10) close to the decomposed ones (9) while imposing the exponential stability constraint. Our previous work in [22] synthesized distributed controllers by looking for both output matrices C_{ii} and E_i in (10) which may have a significant number of decision variables and hence, it may result in a large-scale and computationally intensive NLP. The proposed approach, however, significantly reduces the number of parameters to be optimized for the synthesis of distributed controllers. More specifically, we do *not* search for C_{ii} and only focus on E_i.

V. Simulation Results

The objective of this section is to numerically verify the theoretical results for human-robot locomotion. We consider a lower-extremity amputee as the human subsystem and assume that a 3D tree-like structure with square-profile foot represents the human body (see Fig. 2(a), 2(c)). The robot subsystem on the other hand comprises a knee-ankle powered prosthesis where the foot is modeled with a square profile (see Fig. 1). While we model the powered prosthesis after [30], we extend it with an additional "passive" DOF, attributed to the compliance in the ankle roll for simulation purposes. Under this consideration, we assume the entire structure to consist of 19 DOFs. The first 6 DOFs are attributed to the absolute position and orientation of the human body. The remaining 13 DOFs are the internal shaping variables that are distributed between both the legs as follows: 3 DOFs are associated with the hip to model the roll, pitch, yaw angles, one DOF captures the pitch joint at the knee, further 2 DOFs are allocated to the ankle pitch and roll, and one "passive" DOF is employed to model the point of attachment of the prosthesis to the residual human leg. This completes the state vector $x := \text{col}(q, \dot{q}) \in \mathcal{X} \subset \mathbb{R}^{38}$ and the control vector $u \in \mathcal{U} \subset \mathbb{R}^{11}$. We adopt the kinematic and dynamic parameters of [31] and [30] for the human and robot components of the system, respectively.

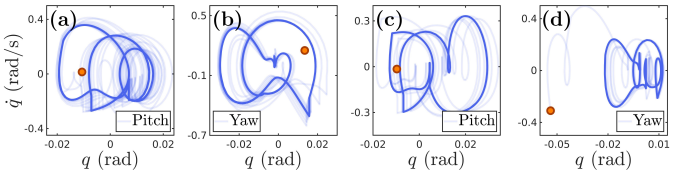

Fig. 3. Phase portraits captured over 100 steps: body's (a) pitch and (b) yaw, as a result of decomposition from a stable centralized orbit. Body's (c) pitch and (d) yaw, as a result of decomposition from an unstable centralized orbit. Here, circles depict the initial conditions.

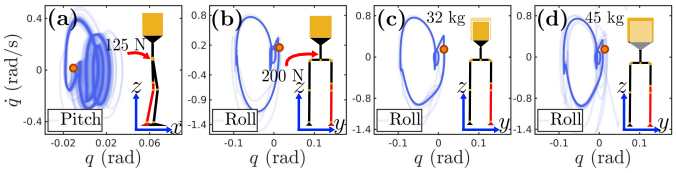

Fig. 4. Robustness phase portraits captured over 100 steps: (a) due to a $\mathbf{125}$ (N) persistent force along the x-axis, (b) due to a $\mathbf{200}$ (N) persistent force along the y-axis, (c) due to a $\mathbf{-8.82}$ (kg) uncertainty in the torso mass, and (d) due to $\mathbf{+4.18}$ (kg) uncertainty in the torso mass.

In this paper, we consider a 4-domain walking cycle to include flat-footed phases (domains v_1 and v_3) and push-off phases (domains v_2 and v_4) that mimic natural human walking (see Fig. 2(b)). With this directed graph, we formulate an optimization problem via FROST [32] to solve for two different desired periodic gaits, $\mathcal{O}$ with a speed of 0.2 (m/s) and 0.3 (m/s). To demonstrate the power of the proposed approach in synthesizing local controllers, we first design centralized controllers as in (4) such that the 0.2 (m/s) and 0.3 (m/s) gaits becomes stable and unstable, respectively.

We then systematically proceed with the proposed decomposition approach by separating the human-robot system into two discrete subsystems at the point of severance, located just above the left knee. The human subsystem Σ_1 retains the base DOFs in addition to its 9 DOFs which results in $\dim(x_1) = 30$ and $\dim(u_1) = 9$. Similarly, the robotic subsystem Σ_2 has 4 DOFs with two passive joints, including the ankle roll and point of attachment of two subsystems, i.e., $\dim(x_2) = 8$ and $\dim(u_2) = 2$. In addition, we utilize a set of global position and velocity variables, $\psi_2(q)$ and $\dot{\psi}_2(q, \dot{q})$, that are obtained from a "*single*" IMU located on the residual human thigh. The human subsystem has no avail of the global IMU variables, indicating that $\psi_1 = \emptyset$ as it already has access to its own absolute position and orientation. We remark that in this formulation, the local controller for the robotic subsystem in (10) has access to *at most* 14 state variables. This is a direct result of its 8 internal states and the availability of *at most* 6 global variables from the IMU in the form of $\psi : \{r, p, y\}$ and $\dot{\psi} : \{\dot{r}, \dot{p}, \dot{y}\}$, in which r, p, y denote the roll, pitch, and yaw angles, respectively. Likewise, local controller for the human subsystem in (10) has access to *at most* 30 state variables.

The entire mechanical system has 8 DOFs during the push-off phases and 13 DOFs during the flat-footed phases. In order to have a nontrivial zero dynamics, we consider 7-dimensional and 11-dimensional outputs (3) in push-off and flat-footed phases, respectively. We then decompose y into (y_1, y_2) such that y_1 includes the DOFs assigned to the human subsystem and y_2 includes the ones for the robotic subsystem. We remark that for the push-off domains (v_1 and v_3), $\dim(y_1) = 6$ and $\dim(y_2) = 1$, and the corresponding decoupling matrices in (13) become $A_1 \in \mathbb{R}^{6\times 9}$ and $A_2 \in \mathbb{R}^{1\times 2}$. In addition for the flat-footed domains (v_2 and v_4), $\dim(y_2) = 9$, $\dim(y_2) = 2$, $A_1 \in \mathbb{R}^{9\times 9}$, and $A_2 \in \mathbb{R}^{2\times 2}$. Next, we parameterize the local outputs for the robotic subsystem but *not* the human subsystem as (10) by output matrices E_2 over three domains. Here, we assume a local output regulating controller for the human subsystem as [22], [33]. In our parameterization, the Poincaré map is only parameterized by *four* parameters related to the robotic subsystem, i.e., $\xi \in \mathbb{R}^4$, whereas the synthesis problem in [22, Sec. VII.B] included 78 parameters for a model with *less DOFs* (i.e., 94.8% *reduction in controller parameters*). The local parameters for the robotic leg are then effectively optimized by the NLP (16) for exponential stability. Here the Poincaré section is taken at the beginning of domain v_1 and the Poincaré map is $15 = 2 \times 8 - 1$ dimensional as the mechanical system has 8 DOFs in domain v_1. In addition, we make use of a total of four parameters to parameterize the local outputs over three domains. The four optimal values of E_2 are $\{0.0571, 0.1017, -0.4186, 2.0232\}$ that correspond to the IMU pitch, roll, pitch, and yaw, respectively (see [34]). Figure 3(a)-(b) illustrates the phase portraits for the human pitch and yaw angles, respectively, over 100 consecutive steps for the 0.2 (m/s) gait. Convergence to the periodic orbit is clear. To show that the distributed architecture does *not* rely on the existence of a stabilizing centralized controller, we repeat the same procedure for the 0.3 (m/s) gait with an unstable centralized controller. Figures 3(c)-(d) demonstrate the distributed controller's ability to stabilize the gait despite having an originally unstable centralized controller.

Robustness Analysis: To illustrate robustness against external disturbances, we induce persistent forces during the prosthetic leg's swing phase (v_2) for every step taken. First, a persistent force of 125 (N) is exerted along the x-axis. In an other simulation, a persistent force of 200 (N) is applied in the direction of negative y-axis. Figures 4(a)-(b) demonstrate convergence to a stable orbit indicating the controller's positive response to the provided disturbances. Furthermore, to show the controller's robustness to uncertainties in dynamic parameters, we vary the mass of the torso while still employing the distributed controller synthesized with the original torso mass of 40.82 (kg). Two simulations, one with torso mass of 32 (kg) and the other with torso mass of 45 (kg), demonstrate stability by converging to periodic orbits as illustrated in Figs. 4(c)-(d).

To draw meaningful differences between the existing centralized and the proposed distributed controllers, we induce white Gaussian noise with a signal-to-noise-ratio (SNR) of 42 (db) into the velocity components of the actuated prosthesis DOFs. Figures 5(a)-(b) show torques captured over one step in the human subsystem for the centralized and distributed control frameworks, respectively. It can be seen from Fig. 5(a) that the induced sensor noise in the prosthesis joints propagates and manifests itself in the joint torques of the human subsystem under the centralized architecture. However, joint torques in the human subsystem are unaffected under the distributed framework (see Fig. 5(b)). Additionally, we note that the amplitude of noise is significantly higher in the centralized control framework. The animations of all

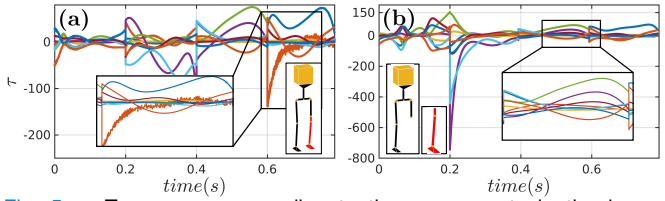

Fig. 5. Torques corresponding to the components in the human subsystem under the (a) centralized control scheme and (b) distributed control scheme.

simulations together with the optimal modified outputs can be found online [34].

VI. Conclusions

This paper established a formal foundation, based on decomposition, HZD, and optimization, to synthesize distributed controllers for exponential stabilization of cooperative human-robot locomotion. The proposed approach assumes a set of HZD-based centralized controllers and then decomposes the dynamics and virtual constraints while parameterizing them with some adjustable local parameters. This decomposition method significantly reduces the parametric space resulting in a small-scale optimization problem compared to previous approaches for synthesizing local controllers. Furthermore, the Poincaré map for the closed-loop hybrid models of locomotion with distributed controllers is investigated and compared to that with centralized ones. We numerically validated the proposed distributed scheme for stable, robust, and multi-domain human-robot locomotion with a powered prosthetic leg and 19 DOFs. For future research, we will investigate the design of robust distributed controllers for locomotion on rough terrains. We will also experimentally evaluate the approach on powered prosthetic legs attached to lower limb amputees.

References

[1] M. F. Eilenberg, H. Geyer, and H. Herr, "Control of a powered ankle–foot prosthesis based on a neuromuscular model," *IEEE transactions on neural systems and rehabilitation engineering*, vol. 18, no. 2, pp. 164–173, 2010.

[2] F. Sup, H. A. Varol, and M. Goldfarb, "Upslope walking with a powered knee and ankle prosthesis: initial results with an amputee subject," *IEEE transactions on neural systems and rehabilitation engineering*, vol. 19, no. 1, pp. 71–78, 2010.

[3] A. M. Simon, K. A. Ingraham, N. P. Fey, S. B. Finucane, R. D. Lipschutz, A. J. Young, and L. J. Hargrove, "Configuring a powered knee and ankle prosthesis for transfemoral amputees within five specific ambulation modes," *PloS one*, vol. 9, no. 6, p. e99387, 2014.

[4] J. Grizzle, G. Abba, and F. Plestan, "Asymptotically stable walking for biped robots: Analysis via systems with impulse effects," *IEEE Transactions on Automatic Control*, vol. 46, no. 1, pp. 51–64, Jan 2001.

[5] A. Ames, K. Galloway, K. Sreenath, and J. Grizzle, "Rapidly exponentially stabilizing control Lyapunov functions and hybrid zero dynamics," *IEEE Transactions on Automatic Control*, vol. 59, no. 4, pp. 876–891, April 2014.

[6] M. Spong and F. Bullo, "Controlled symmetries and passive walking," *IEEE Transactions on Automatic Control*, vol. 50, no. 7, pp. 1025–1031, July 2005.

[7] I. Manchester, U. Mettin, F. Iida, and R. Tedrake, "Stable dynamic walking over uneven terrain," *The International Journal of Robotics Research*, vol. 30, no. 3, pp. 265–279, 2011.

[8] G. Song and M. Zefran, "Underactuated dynamic three-dimensional bipedal walking," in *Proceedings IEEE International Conference on Robotics and Automation*, May 2006, pp. 854–859.

[9] A. M. Johnson, S. A. Burden, and D. E. Koditschek, "A hybrid systems model for simple manipulation and self-manipulation systems," *The International Journal of Robotics Research*, vol. 35, no. 11, pp. 1354–1392, 2016.

[10] R. Vasudevan, "Hybrid system identification via switched system optimal control for bipedal robotic walking," in *Robotics Research*. Springer, 2017, pp. 635–650.

[11] A. D. Ames, R. D. Gregg, E. D. B. Wendel, and S. Sastry, "On the geometric reduction of controlled three-dimensional bipedal robotic walkers," in *Lagrangian and Hamiltonian Methods for Nonlinear Control 2006*. Berlin, Heidelberg: Springer, 2007, pp. 183–196.

[12] R. D. Gregg and M. W. Spong, "Reduction-based control of three-dimensional bipedal walking robots," *The International Journal of Robotics Research*, vol. 29, no. 6, pp. 680–702, May 2010.

[13] A. Shiriaev, L. Freidovich, and S. Gusev, "Transverse linearization for controlled mechanical systems with several passive degrees of freedom," *IEEE Transactions on Automatic Control*, vol. 55, no. 4, pp. 893–906, April 2010.

[14] E. Westervelt, J. Grizzle, and D. Koditschek, "Hybrid zero dynamics of planar biped walkers," *IEEE Transactions on Automatic Control*, vol. 48, no. 1, pp. 42–56, Jan 2003.

[15] S.-H. Wang and E. Davison, "On the stabilization of decentralized control systems," *IEEE Transactions on Automatic Control*, vol. 18, no. 5, pp. 473–478, Oct 1973.

[16] R. Lau, R. Persiano, and P. Varaiya, "Decentralized information and control: A network flow example," *IEEE Transactions on Automatic Control*, vol. 17, no. 4, pp. 466–473, 1972.

[17] D. Siljak, *Decentralized Control of Complex Systems*. Dover Publications, December 2011.

[18] A. Agrawal, O. Harib, A. Hereid, S. Finet, M. Masselin, L. Praly, A. D. Ames, K. Sreenath, and J. W. Grizzle, "First steps towards translating hzd control of bipedal robots to decentralized control of exoskeletons," *IEEE Access*, vol. 5, pp. 9919–9934, 2017.

[19] A. E. Martin and R. D. Gregg, "Stable, robust hybrid zero dynamics control of powered lower-limb prostheses," *IEEE Transactions on Automatic Control*, vol. 62, no. 8, pp. 3930–3942, 2017.

[20] R. Gregg, T. Lenzi, L. Hargrove, and J. Sensinger, "Virtual constraint control of a powered prosthetic leg: From simulation to experiments with transfemoral amputees," *IEEE Transactions on Robotics*, vol. 30, no. 6, pp. 1455–1471, Dec 2014.

[21] R. Gehlhar and A. D. Ames, "Separable control lyapunov functions with application to prostheses," *IEEE Control Systems Letters*, vol. 5, no. 2, pp. 559–564, 2020.

[22] K. Akbari Hamed and R. D. Gregg, "Decentralized feedback controllers for robust stabilization of periodic orbits of hybrid systems: Application to bipedal walking," *IEEE Transactions on Control Systems Technology*, vol. 25, no. 4, pp. 1153–1167, July 2017.

[23] ——, "Decentralized event-based controllers for robust stabilization of hybrid periodic orbits: Application to underactuated 3D bipedal walking," *IEEE Transactions on Automatic Control*, vol. 64, no. 6, pp. 2266–2281, June 2019.

[24] A. Pandala, V. R. Kamidi, and K. Akbari Hamed, "Decentralized control schemes for stable quadrupedal locomotion: A decomposition approach from centralized controllers," in *IEEE/RSJ International Conference on Intelligent Robots and Systems (IROS)*, Oct 2020, pp. 3975–3981.

[25] Y. Hurmuzlu and D. B. Marghitu, "Rigid body collisions of planar kinematic chains with multiple contact points," *The International Journal of Robotics Research*, vol. 13, no. 1, pp. 82–92, 1994.

[26] A. Isidori, *Nonlinear Control Systems*. Springer; 3rd edition, 1995.

[27] H. K. Khalil, *Nonlinear Systems*. Pearson, 3rd edition, 2001.

[28] J. Martin, V. R. Kamidi, A. Pandala, R. Fawcett, and K. Akbari Hamed, "Exponentially stabilizing and time-varying virtual constraint controllers for dynamic quadrupedal bounding," in *IEEE/RSJ International Conference on Intelligent Robots and Systems (IROS)*, Oct 2020, pp. 3914–3921.

[29] T. Parker and L. Chua, *Practical Numerical Algorithms for Chaotic Systems*. Springer, 1989.

[30] T. Elery, S. Rezazadeh, C. Nesler, and R. D. Gregg, "Design and validation of a powered knee–ankle prosthesis with high-torque, low-impedance actuators," *IEEE Transactions on Robotics*, vol. 36, no. 6, pp. 1649–1668, 2020.

[31] P. de Leva, "Adjustments to Zatsiorsky-Seluyanov's segment inertia parameters," *J Biomech*, vol. 29, no. 9, pp. 123–1230, 1996.

[32] A. Hereid and A. D. Ames, "FROST: Fast robot optimization and simulation toolkit," in *IEEE/RSJ International Conference on Intelligent Robots and Systems (IROS)*, Sep 2017, pp. 719–726.

[33] D. J. Villarreal, H. A. Poonawala, and R. D. Gregg, "A robust parameterization of human gait patterns across phase-shifting perturbations," *IEEE Transactions on Neural Systems and Rehabilitation Engineering*, vol. 25, no. 3, pp. 265–278, March 2017.

[34] [Online]. Available: https://youtu.be/MiGhjggJhpI